Acta Oceanol. Sin., 2023, Vol. 42, No. 8, P. 99–112
https://doi.org/10.1007/s13131-023-2235-1
http://www.aosocean.com
E-mail: ocean2@hyxb.org.cn

Phosphorus speciation, transformation and benthic processes with implications for environmental impacts in the aquaculture area of Rushan Bay

Yao Feng[1†], Jun Liu[1, 2*†], Aijun Zhang[1], Yibin Wang[1], Lu Wang[2], Zongqing Lv[1], Xiangbin Ran[1, 2]

[1] Marine Ecology Research Center/Key Laboratory of Marine Eco-Environmental Science and Technology, First Institute of Oceanology, Ministry of Natural Resources, Qingdao 266061, China

[2] Laoshan Laboratory, Qingdao 266237, China

Received 13 March 2023; accepted 27 June 2023

Abstract

Phosphorus (P) is an essential nutrient for many organisms in the ocean, which plays a central role in the stability of ecosystems and the evolution of the environment. The distribution, occurrence and source-sink process of P in offshore waters are highly influenced by mariculture activities. P transformation in water-sediment system is the key process in P cycling, however, the mechanism is poorly documented in the coastal sea which is influenced by human activities. Based on the comprehensive surveys in the adjacent waters outside Rushan Bay in May, July and August 2014 and February 2015, the form and transformation of P in the suspended particulate matter (SPM) and surface sediment were analyzed. The results showed that contents of total P, authigenic P and organic P of SPM increased with the increase in distance from the shoreline off Rushan Bay, and the detrital-P decreased. The partition coefficient of P between water and SPM was related to the chemical activity of different forms of P, and a higher reactivity of inorganic P associated with SPM was observed. Hypoxia induced by mariculture changes the distribution and morphological composition of P in SPM and sediment in this typical aquaculture area, which can result in a conversion of sink to source of P in the sediment, thereby having a significant impact on the regional nutrient budget and associated with eutrophication.

Key words: phosphorus speciation, transformation, benthic process, aquaculture, Rushan Bay

Citation: Feng Yao, Liu Jun, Zhang Aijun, Wang Yibin, Wang Lu, Lv Zongqing, Ran Xiangbin. 2023. Phosphorus speciation, transformation and benthic processes with implications for environmental impacts in the aquaculture area of Rushan Bay. Acta Oceanologica Sinica, 42(8): 99–112, doi: 10.1007/s13131-023-2235-1

1 Introduction

Phosphorus (P) is the main limiting nutrient in most environments and plays a key role in maintaining the stability of marine ecosystems (Duhamel et al., 2021). With the economic development and enhanced human activities, a large number of land-based pollutants enter the coastal sea, thereby changing the level and structure of nutrients in the offshore waters worldwide. Different from other macro-nutrient elements such as nitrogen (N), P has high particle reactivity and is mainly present in colloidal and granular forms in the natural water. The changes in the occurrence of P are the key factors affecting P cycling. Different forms of P have different bioavailability, which is likely to cause changes in different water environments (Defforey and Paytan, 2018; Duhamel et al., 2021). Previous studies have also found that total P (Tot-P) cannot completely predict the potential benthic flux or chemical activity of sediment as an internal load P source, and the insight of occurrence of different P loading in sediment is thus more critical than its bulk abundance (Asmala et al., 2017; Ballagh et al., 2021; Liu et al., 2022).

The interaction between sediment and water body mainly controls the P biogeochemical process. Sediment is a key sink of P in many marine systems by burying a certain amount of particulate P. At the same time, sediment regulates the P level in water through resuspension, early diagenetic process, and bottom interface diffusion (Leote and Epping, 2015; Liu et al., 2020), these above processes are largely controlled by the dissolved oxygen (DO) level in the water environment (Lin et al., 2016) and also serves as the source of P for water column.

Previous studies have found that cage culture could accelerate organic matter pollution and eutrophication in aquaculture waters (Islam, 2005; Zhang et al., 2022; Go et al., 2023), and the biogeochemical cycle of P in the mariculture area was different from that in other coastal area due to its difference in source (Zhang et al., 2022; Dong et al., 2022). The potential ecological impact of regional P cycle changes thus needs further study. However, the major processes of P cycle in the mariculture area are unclear.

Rushan Bay and its offshore area are an important economic shellfish culture area with extensive tidal flat, fertile water quality and clay silt as the main substrate. High density breeding may enhance water deoxygenation, which would inevitably affect regional P cycle (Wang et al., 2009; Liu et al., 2016), especially under seasonal low oxygen conditions. This research chooses an offshore area of Rushan Bay, a typical nearshore culture zones in

Foundation item: The National Natural Science Foundation of China under contract Nos 41806097, 42176048 and 42149902.
*Corresponding author, E-mail: liu009@fio.org.cn
†These authors contributed equally to this work.

Shandong Peninsula, and sampled in different seasons considering seasonal hypoxia. The major objectives are: (1) explore the major transformation processes of P between water and sediment; (2) evaluate the effect of DO level on P cycling in mariculture environment. This study would provide a scientific basis for environmental management in the typical aquaculture area.

2 Materials and methods

2.1 *Study area*

Rushan Bay (36°44′–36°52′N, 121°25′–121°37′E) is located in the coastal area of the southern Shandong Peninsula, and connected to the South Yellow Sea. Rushan Bay is a half closed shallow bay, and the water mass in the study area is affected by the Yellow Sea Coastal Current (Liu et al., 2016). The main river in the study area is the Rushan River, with a total length of about 64 km (Liu et al., 2015). The depth of the study area off Rushan Bay ranges from 5 m to 30 m (Fig. 1) with a fairly frequency water exchange and great influence of water environment from the Rushan Bay.

Rushan Bay including its adjacent coastal area is an important economic shellfish aquaculture area. With the development of industry, agriculture and aquaculture in recent years, the large amount of N and P nutrients input has led to a series of changes in the water quality and environment, such as the obvious trend of eutrophication (He et al., 2017) and seasonal hypoxia in the coastal area of Rushan Bay (Liu et al., 2016).

2.2 *Sample collection and pretreatment*

In May (spring), July (summer), August (summer) 2014 and February (winter) 2015, four comprehensive surveys were conducted in the adjacent waters of Rushan Bay. The sampling stations are shown in Fig. 1. The temperature (T), salinity (S) and DO of the site were obtained using a thermosaline-deep multiparameter water quality analyzer (JFE Co. Ltd, AAQ122, Japan). Water samples were collected by Niskin collector at the surface (the surface depth was generally set at 0.5 m below water surface) and near the bottom layer (2 m above seabed). DO was titrated using the Winkler method using a Coulomb Titrino (Metrohm, 877 Titrino Plus, Switzerland).

A certain volume of the bottom water sample was filtered with a 0.45 μm pore size polyethersulfone filter (PES filter) (presoaked with a volume ratio of 1:1 000 HCl for 24 h, washed with Milli-Q to neutral, dried and weighed at 45℃). We separated the filtrate using polyethylene bottles (the sample bottles were soaked in 1:5 HCl for more than 48 h, and then washed several times with Milli-Q water to neutral) and frozen them at –20℃ before nutrient determination. Another certain volume of filtrate was divided into 10 mL polystyrene bottles (soaked in 1:5 HCl for more than 48 h in advance, cleaned with Milli-Q water to neutral), and acidified with pure nitric acid to pH<1, stored at 4℃ for analysis of dissolved Fe and Mn. In addition, a certain volume of the overlying water sample was filtered with GF/F filter membrane. The membrane samples were quickly protected from light and freeze-dried for the analysis of chlorophyll *a* (Chl *a*) in water. The 25 L bottom water was filtered by 0.45 μm acetate fiber filter membrane (pretreatment was the same as the PES filter above) to collect deposited/suspended particulate matter (SPM). The filter volume of the water sample was recorded and the membrane was placed in a membrane box and frozen (–20℃) for determination of particulate P form, total organic carbon (TOC) and total organic nitrogen (TON).

Sediments were collected by a box type mud harvester. Surface sediments (0–2 cm) were scraped into sealed bags after the overlying water was removed, filled with N_2 and stored at 4℃ for analysis of different forms of P in sediments. Another part of the surface sediment sample, frozen at –20℃, was used to analyze TOC content in the sediment.

2.3 *Process of culture experiment*

The detailed procedure of culture experiment was described in Liu et al. (2016). Briefly, the experiment was divided into three groups: oxygen-rich (6.8 mg/L), hypoxic (2.0 mg/L) and anaerobic (quasi-anaerobic, <0.1 mg/L), which was implemented in the portable multiple sediment-seawater corer incubation system (Liu et al., 2016). The treated bottom seawater was slowly injected into the upper end of the culture tube. The peristaltic pump was used to control the turnover time of overlying water in the culture unit close to the actual field flow condition. The overlying water DO concentration was kept at a stable level through controlling the volume ratio of nitrogen and oxygen injection. The culture experiment was carried out at constant tem-

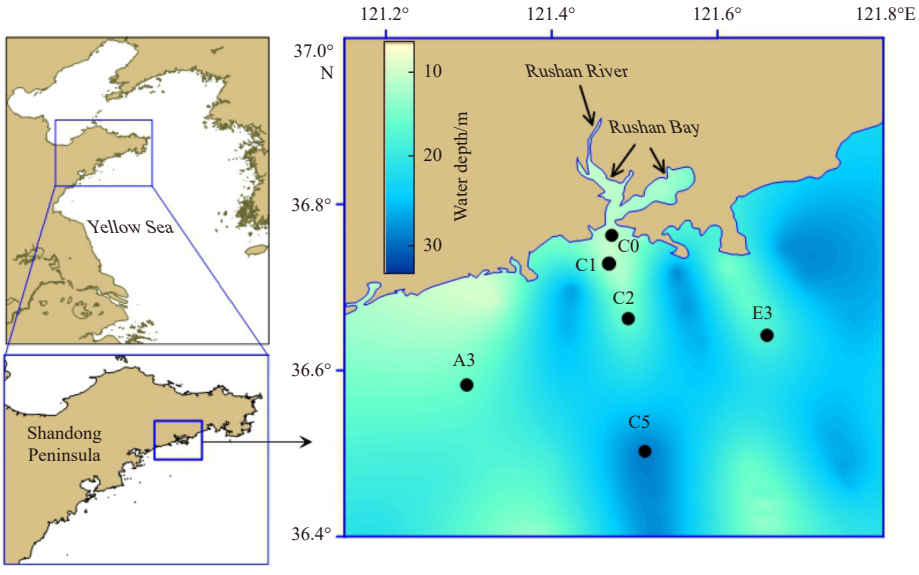

Fig. 1. Sampling stations in the adjacent area of Rushan Bay (water depth is described from the data of the depth sounder on board).

perature and away from light. During culture, overlying water samples were taken every 1–2 d and cultured continuously for 12 d. After the sampling was completed, the filtered bottom seawater was added according to the above sampling method, so that the upper end of the culture tube was filled with the overlying water again, and the next stage of the experiment was carried out.

2.4 *Laboratory analyses*

2.4.1 *Water samples analyses*

The water samples of each layer were filtered by 0.45 μm acetate fiber filtration membrane. Dissolved inorganic nitrogen (DIN) and dissolved reactive phosphorus (DRP) in water samples were determined using an automatic nutrient analyzer (SEAL Analytical Gmbh, QuAAtro, Germany) with the detection limits as follows: Nitrate (NO_3^-, in N, the same below) is 0.015 μmol/L, nitrite (NO_2^-) is 0.003 μmol/L, ammonia nitrogen (NH_4^+) is 0.040 μmol/L, DRP is 0.024 μmol/L, relative standard deviation <0.3%. DIN concentration is the sum of NO_3^-, NO_2^- and NH_4^+. Chl *a* was determined by fluorescence spectrophotometry. The samples were extracted with 90% acetone at low temperature (4℃) in dark for 18–24 h and then determined by fluorescence spectrophotometer (Shanghai Instrument, 970CRT, China). The dissolved Fe and Mn in water samples were determined by ICP-MS (Agilent, 7500A, America), and the measurement errors were less than 5%. All dissolved Fe and Mn in interstitial water are expressed as Fe^{2+} and Mn^{2+} (Mort et al., 2010).

2.4.2 *Particulate matter and sediment analyses*

The grain sizes of the particulate and sediment samples were determined using a laser particle size analyzer (Mastersizer 2000, Malvern Instruments Ltd., UK) (Liu et al., 2016). The particle sizes for clay, silt and sand were <4 μm, 4–63 μm, and >63 μm, respectively, and their values were shown as percentage.

The sediment samples were dried at low temperature (45℃) using oven (Aoxi, WGLL-125BE, China), ground and passed through a 200-mesh screen. After fully mixing, about 0.5 g of sediment samples were added to 5 mL of 1 mol/L HCl and soaked for 12 h. Then, new HCl solution was added until no bubbles emerged (Jilbert and Slomp, 2013). The sediment was dried at low temperature and weighted at constant weight. The approximately 15 mg sediment sample was weighted and enclosed it in a tin cup for testing. The percentage TOC and TON contents of sediment samples were obtained by weight difference correction before and after pickling (Poulton and Canfield, 2005).

The treatment method of organic carbon in SPM was based on the following procedures. The filter membrane was dried at 45℃ in the oven, and then weighed after 48 h of constant weight in the dryer. The dried membrane was acid-smoked for 48 h with hydrochloric acid vapor to remove inorganic carbon. The membrane was repeatedly rinsed with Milli-Q water until neutral. The filters were dried at low temperature and weighted at constant weight, and then the acid-dried membrane was wrapped in a tin cup.

Organic carbon in sediments and SPM was determined using an elemental analyzer (EURO, EA3000, Germany) with a relative standard deviation of less than 10%.

The pretreatment method is the same as the pretreatment method of organic carbon in SPM. $\delta^{13}C$ in the sample was determined using a Carlo Erba NA 1 500 Series elemental analyzer (Fisons Instruments, USA) connected to a DELTA PLUS^{XP} continuous flow isotope ratio mass spectrometer (Thermo Finnigan Instruments, USA). The reference standard for the $\delta^{13}C$ value adopts the Vienna Peedee Belemnite (VPDB) international standard and is calculated according to the following formula:

$$\delta^{13}C\,(‰) = \left[\frac{R\left(^{13}C/^{12}C_{sample}\right)}{R\left(^{13}C/^{12}C_{VPDB}\right)} - 1\right] \times 1\,000, \tag{1}$$

where $R(^{13}C/^{12}C_{VPDB})$ is the carbon isotope abundance ratio of the international standard substance VPDB, and $R(^{13}C/^{12}C_{sample})$ is the carbon isotope abundance ratio of the sample.

The TOC contribution from terrestrial inputs (W_T, %) was determined based on the carbon isotopic balance model according to Wu et al. (1999):

$$W_T = (\delta^{13}C - \delta^{13}C_M)/(\delta^{13}C_T - \delta^{13}C_M), \tag{2}$$

where $\delta^{13}C_M$ (−19.5‰) and $\delta^{13}C_T$ (−27‰) are the $\delta^{13}C$ values of material with marine and terrestrial origins, respectively (Wu et al., 1999).

SPM and surface sediment samples were freeze-dried using a vacuum freezing dryer (Yuane, DF-1A-50, China), ground in an agate bowl and mixed. Accurate weighing of 0.1 g was used to analyze the occurrence and form of P in particulate matter. A wet sample of 0.1 g of surface sediment was used for the analysis of P forms. Analysis of the occurrence form of P in SPM and sediment were fractionated by the chemical continuous extraction method (SEDEX) (Ruttenberg, 1992; Liu et al., 2016). The particulate P was divided into five forms: exchangeable phosphorus (Exch-P), iron-bound phosphorus (Fe-P), authigenic P (Auth-P), detrital-P (Det-P) and organic P (Org-P). The Tot-P was the sum of each form of P in content. The sum of Exch-P, Fe-P and Org-P were defined as bioavailable P. During the determination of P, blank samples (reagents used in the SEDEX sequential P extraction scheme), parallel samples and reference materials (0.1 g of China offshore sediment standard (GBWO7314)) were extracted simultaneously to ensure the accuracy of the analysis results.

The DRP obtained after extraction was determined by phosphorus-molybdenum blue-spectrophotometry, and the analytical method was the same as that of water sample. And the solution after sodium citrate-dithionite-bicarbonate (CDB) extraction in step 2 of the SEDEX procedure was divided into two parts, one for P measurement and the other for iron and manganese measurement after acidification with pure nitric acid. Fe and Mn in CDB solution were determined by flame atomic absorption spectrophotometer (Varian, AA140/240, America), and the relative standard deviation of multiple measurements was less than 10%. The Fe and Mn analyzed in this process are reducible amorphous or weakly amorphous oxides or hydroxides, denoted respectively as Fe_{CDB} and Mn_{CDB}.

2.5 *Data processing*

2.5.1 *Calculation of the partition coefficient of solid and liquid phase P*

Partitioning coefficient (K_d) is widely used in aquatic ecosystems to quantitatively describe the partitioning behavior of dissolved P and particulate P and the activity of particulate P (Lin et al., 2016). K_d was calculated by the following formula:

$$K_d = \frac{C_p}{C_d \times [SPM]}, \tag{3}$$

where C_p is the concentration of particulate P (μmol/L); C_d is the concentration of dissolved inorganic P (DIP) (μmol/L); and [SPM] is the concentration of SPM (g/L). The unit of K_d is L/g. The K_d of total particulate P (TPP), particulate organic P (POP) and particulate inorganic P (PIP) was calculated by the Eq. (5) when C_p replaced by the concentrations of TPP, POP, and PIP (μmol/L), respectively.

2.5.2 *Phosphorus loss from sediment during culture experiments*

$$P_{loss} = \int_0^z S\rho\,(C_i - C_0)\,dz, \tag{4}$$

where P_{loss} is the total phosphorus lost (μmol) in sediments after culture experiment; S is the cross-sectional area (cm^2) of the culture tube; ρ is the dry density (g/cm^3) of the sediment; C_0 and C_i (μmol/g) are the P contents before and after sediment culture, respectively; z is the sediment depth (cm).

2.5.3 *Data processing method*

Statistical analysis was performed using SPSS 18 (IBM Corporation, USA) for Pearson correlation analysis between parameters (two-tailed test) and significant difference analysis between data (one-tailed test). Graphic description and analysis were used by Origin 2019 (OriginLab Corporation, USA).

3 Results

3.1 *DO, Chl a, dissolved nutrient, iron and manganese in water column*

DO ranges from 120 μmol/L to 370 μmol/L, and DO saturation ranged from 41% to 130% (Table 1), indicating that there are significant seasonal differences in DO in the bottom water in the study area, and DO had a seasonal alternating state of deficit or saturation. The concentration of Chl *a* in water ranged from 0.10–4.1 μg/L, and the difference in seasonal variation of Chl *a* was small (Table 1). The concentration of DRP in water ranged from 0.10 μmol/L to 0.44 μmol/L (Table S1), with significant seasonal differences, with higher concentration in summer and lower concentration in winter. The mole ratio of DIN to DRP was averaged 20:1, showing potential P limitation relative to Redfield ratio (16:1). The concentration of Fe^{2+} in water ranged from 134 nmol/L to 919 nmol/L, and the concentration of Mn^{2+} in water varied from 6.5 nmol/L to 77 nmol/L. The concentration of Fe^{2+} was high in August and low in February. The seasonal difference of Mn^{2+} was small.

3.2 *Organic carbon, nitrogen, iron and manganese oxides in SPM and sediment*

The variation range of TOC and TON in SPM was 0.50%–1.1% and 0.10%–0.19%, respectively. There were no significant seasonal differences in TOC and TON in SPM (Table 2, Table S2). The variation range of TOC in sediments was 0.40%–0.88%. The range of TON was 0.10%–0.17%. There were no significant seasonal differences in TOC and TON in sediments. TOC content in sediment matter was higher than that in suspended particle, and TON content was close to that in suspended matter.

The variation range of Fe_{CDB} in SPM was 36–48 μmol/g. Fe_{CDB} content was relatively high in August, followed by July, and relatively low in May. The variation range of Mn_{CDB} was 7.2–11 μmol/g, and the seasonal difference of Mn_{CDB} content was not significant. The range of Fe_{CDB} in surface sediments as 25–78 μmol/g. Fe_{CDB} content was relatively high in August, followed by July, and relatively low in May. The variation range of Mn_{CDB} was 2.0–18 μmol/g, and the seasonal difference of Mn_{CDB} content was not significant. The contents of Fe_{CDB} and Mn_{CDB} in SPM and sediments were similar, but the range of Fe_{CDB} and Mn_{CDB} in sediments was large.

3.3 *Phosphorus speciation in SPM and sediment*

The variation range of Tot-P in SPM was 13–28 μmol/g. Inorganic P was the main component of Tot-P, accounting for 77% ± 5% of Tot-P on average, while Org-P accounted for a small proportion (Table 3, Table S2). The mean value of Exch-P was (0.52 ± 0.26) μmol/g and the Fe-P was (6.5 ± 2.1) μmol/g. The seasonal variation of Exch-P and Fe-P was significantly different. The mean values of Auth-P, Detr-P and Org-P were (2.1 ± 1.2) μmol/g, (7.7 ± 1.9) μmol/g, and (5.0 ± 1.3) μmol/g, respectively. There was no significant difference in the seasonal variation of these three P forms ($p < 0.5$). In the composition of P, Det-P accounted for the highest percentage of Tot-P, with an average of 35% ± 8.9%, followed by Fe-P, with an average of 30% ± 9.5%. The average proportion of Org-P, Auth-P and Exch-P in Tot-P was 23% ± 5.9%, 9.6% ± 5.5% and 2.4% ± 1.2%, respectively. The contribution of bioavailable P to Tot-P was 55%.

The variation of Tot-P in surface sediments ranged from 13 μmol/g to 19 μmol/g, and inorganic P was the main component of Tot-P, accounting for 82% ± 5% of Tot-P on average, while Org-P accounted for a small proportion. The mean values of Exch-P, Fe-P, Auth-P, Det-P and Org-P were (0.23 ± 0.10) μmol/g,

Table 1. Overlying water and sediment sampling sites and characteristics presented in this study

	February 2015		May 2014		July 2014		August 2014	
	Range	Mean	Range	Mean	Range	Mean	Range	Mean
Depth/m	6.00–13.0	9.67 ± 3.51	8.61–28.9	15.6 ± 7.86	8.88–22.6	16.5 ± 5.12	4.60–29.7	17.2 ± 8.69
Temperature/℃	3.30–3.40	3.33 ± 0.06	11.2–16.4	14.2 ± 2.00	15.9–24.7	20.7 ± 3.41	20.0–26.9	23.1 ± 2.38
Salinity	31.4–31.5	31.4 ± 0.06	30.6–31.0	30.8 ± 0.13	30.8–30.9	30.8 ± 0.05	29.8–30.8	30.5 ± 0.38
DO concentration/($mg{\cdot}L^{-1}$)	10.9–11.5	11.2 ± 0.30	8.19–9.32	8.71 ± 0.51	5.42–6.02	5.75 ± 0.25	3.75–7.43	4.92 ± 1.29
Chl *a* concentration/($\mu g{\cdot}L^{-1}$)	ND	ND	0.16–2.36	1.19 ± 0.90	0.10–4.08	1.08 ± 1.57	0.10–3.03	1.11 ± 1.08
DRP concentration/($\mu mol{\cdot}L^{-1}$)	0.10–0.19	0.14 ± 0.04	0.12–0.23	0.16 ± 0.04	0.11–0.38	0.19 ± 0.10	0.26–0.44	0.35 ± 0.06
Fe^{2+} concentration/($nmol{\cdot}L^{-1}$)	165–190	179 ± 12.7	134–426	273 ± 122	237–739	367 ± 185	247–919	644 ± 280
Mn^{2+} concentration/($\mu mol{\cdot}L^{-1}$)	6.51–13.4	8.86 ± 3.92	6.93–36.7	25.2 ± 11.6	7.39–67.9	24.7 ± 23.3	13.4–77.0	42.4 ± 25.2
DIN concentration/($\mu mol{\cdot}L^{-1}$)	4.28–11.4	6.66 ± 4.10	1.90–3.61	2.86 ± 0.68	2.02–5.89	3.35 ± 1.35	3.92–6.83	4.93 ± 1.25
N/P molar ratio	ND	ND	6.78–23.6	15.43 ± 8.15	8.16–31.33	20.6 ± 8.20	9.31–20.3	14.3 ± 4.00
Si/P molar ratio	ND	ND	4.88–39.8	23.0 ± 14.5	17.1–98.4	50.9 ± 27.4	26.4–33.2	30.6 ± 3.10

Note: DO: dissolved oxygen; DRP: dissolved reactive P; DIN: dissolved inorganic nitrogen; N/P: ratio of DIN and DRP in water; Si/P: ratio of dissolved silicon and DRP in water; ND: no available data.

Table 2. Range and average of suspended particulate matter (SPM) and surface sediment in the area off Rushan Bay

		May 2014		July 2014		August 2014	
		Range	Mean	Range	Mean	Range	Mean
SPM in overlying water sample	Tot-P content/(μmol·g^{-1})	12.9–21.6	19.1 ± 3.69	18.4–27.4	22.5 ± 3.60	20.3–27.8	23.7 ± 3.20
	Fe_{CDB} content/(μmol·g^{-1})	35.7–39.9	37.3 ± 1.73	37.1–45.10	41.0 ± 3.46	35.6–47.50	42.3 ± 5.51
	Mn_{CDB} content/(μmol·g^{-1})	7.22–9.35	8.26 ± 0.90	8.31–11.15	9.52 ± 0.95	8.35–11.24	9.51 ± 1.07
	TON content/%	0.12–0.15	0.14 ± 0.01	0.12–0.17	0.15 ± 0.02	0.10–0.19	0.15 ± 0.04
	TOC content/%	0.51–0.65	0.61 ± 0.06	0.51–0.93	0.75 ± 0.16	0.50–1.07	0.79 ± 0.20
	δ^{13}C/‰	–22.14–20.40	–21.55 ± 0.47	–21.96–20.97	–21.35 ± 0.53	–21.92–20.39	–21.32 ± 0.51
	C/P molar ratio	92.6–195	122 ± 42.7	105–133	119 ± 10.3	105–144	126 ± 16.6
Surface sediments	Tot-P/(μmol·g^{-1})	12.7–19.3	16.2 ± 2.38	14.6–18.9	16.3 ± 1.49	16.6–19.1	48.5 ± 20.4
	Fe_{CDB}/(μmol·g^{-1})	25.5–46.2	35.7 ± 9.44	27.3–59.1	37.0 ± 11.7	25.2–78.2	48.5 ± 20.4
	Mn_{CDB}/(μmol·g^{-1})	2.04–17.5	8.57 ± 6.55	3.26–11.70	6.88 ± 3.58	3.21–18.1	10.9 ± 6.62
	TON content/%	0.10–0.14	0.13 ± 0.02	0.11–0.17	0.14 ± 0.03	0.10–0.17	0.14 ± 0.03
	TOC content/%	0.40–0.66	0.52 ± 0.09	0.40–0.88	0.67 ± 0.20	0.41–0.74	0.60 ± 0.15
	δ^{13}C/‰	–23.69–21.73	–23.22 ± 0.66	–23.7–21.63	–22.84 ± 0.94	–23.84–21.08	–22.69 ± 0.99
	C/P molar ratio	134–205	167 ± 29.7	136–246	179 ± 41.7	159–279	209 ± 51.0
	Clay/%	12.2–13.7	12.9 ± 1.11	6.13–18.1	15.3 ± 8.11	17.2–26.4	21.3 ± 3.87

Note: SPM is in the overlying water sample. Tot-P: total P; CDB: sodium citrate-dithionite-bicarbonate; TON: total organic nitrogen; TOC: total organic carbon; C/P molar ratio: molar ratio of TOC and Org-P.

Table 3. Contents and seasonal variations of different forms of P in suspended particulate matter (SPM) and surface sediments off Rushan Bay

		SPM					Surface sediment				
		Exch-P/(μmol·g^{-1})	Fe-P/(μmol·g^{-1})	Auth-P/(μmol·g^{-1})	Det-P/(μmol·g^{-1})	Org-P/(μmol·g^{-1})	Exch-P/(μmol·g^{-1})	Fe-P/(μmol·g^{-1})	Auth-P/(μmol·g^{-1})	Det-P/(μmol·g^{-1})	Org-P/(μmol·g^{-1})
May 2014	Range	0.14–0.60	3.74–4.80	1.11–4.04	4.96–10.4	2.76–5.81	0.14–0.26	2.90–4.76	1.42–2.11	4.64–9.83	1.63–3.17
	Mean	0.30 ± 0.19	4.31 ± 0.48	1.96 ± 1.21	8.07 ± 2.26	4.50 ± 1.30	0.19 ± 0.05	3.92 ± 0.79	1.85 ± 0.27	7.57 ± 1.89	2.65 ± 0.60
July 2014	Range	0.27–1.08	5.11–9.11	0.64–3.58	4.67–10.2	4.43–6.84	0.12–0.34	3.52–6.12	0.64–4.00	4.83–9.17	2.07–4.06
	Mean	0.69 ± 0.27	7.06 ± 1.46	1.83 ± 1.07	7.64 ± 2.25	5.25 ± 1.00	0.24 ± 0.09	4.55 ± 1.10	2.12 ± 1.22	6.23 ± 1.57	3.17 ± 0.82
August 2014	Range	0.28–0.67	4.65–10.4	0.98–4.42	5.66–9.46	3.52–7.52	0.19–0.47	4.52–7.49	1.30–2.88	5.03–8.90	1.65–3.98
	Mean	0.54 ± 0.16	7.77 ± 2.08	2.53 ± 1.41	7.56 ± 1.67	5.27 ± 1.61	0.31 ± 0.10	6.10 ± 1.12	2.46 ± 0.59	6.58 ± 1.64	2.45 ± 0.74

Note: SPM is in the overlying water sample. Exch-P: exchangeable phosphorus; Fe-P: iron-bound phosphorus; Auth-P: authigenic P; Det-P: detrital-P; Org-P: organic P.

(4.7 ± 1.4) μmol/g, (2.1 ± 0.75) μmol/g, (6.8 ± 1.6) μmol/g, and (2.9 ± 0.89) μmol/g, respectively, and the seasonal variation of each P fraction was not significant. Det-P accounted for the highest percentage of Tot-P, with an average value of 41% ± 9.6%, followed by Fe-P, with an average value of 28% ± 8.2%. The average proportion of Org-P, Auth-P and Exch-P in Tot-P was 18% ± 5.3%, 13% ± 4.5% and 1.4% ± 0.1%, respectively. The proportion of bioavailable P in Tot-P was averaged 47%.

3.4 *Partitioning of P between dissolved and particulate phases*

The partition coefficient of P between water and particulate matter indicated that the lg K_d value was related to the activity of different forms of P. The lg K_d range of 0.29–2.34 for Tot-P, the lg K_d range of 0.73–2.91 for inorganic P, and the lg K_d range of 0.16–2.24 for Org-P. The distribution coefficient of inorganic P was higher than that of Org-P, reflecting its higher reactivity, which is similar to the observation situation in the Jiulong Estuary and Green Bay, a seasonally low oxygen sea area (Lin et al., 2013, 2016).

4 Discussion

4.1 *Particulate P fractions in the water column*

Suspended particulate matters are important intermediaries in the cycling of P, and other particle-reactive element, due to their high biological and chemical reactivity, resulting in fairly short turnover times and high exchange rates of P in aquatic environments.

Exch-P and Fe-P changed dramatically under the influence of redox environment (Adhikari et al., 2015; Liu et al., 2020). Exch-P is a potentially active P form formed by the direct adsorption of DIP and small molecular Org-P onto the surface of particulate matter, and it is the form with the weakest interaction between particulate matter (Ruttenberg, 1992; Lukkari et al., 2007), which is also an important source of dissolved P in water (Liu et al., 2016). Exch-P, as the active P component adsorbed on the surface of particulate matter (mainly HPO_4^{2-}), is easily replaced by weak organic acids and alkalis (such as OH^-, $HAsO_4^-$, $H_3SiO_4^-$, and F^-) in high salinity seawater (Lukkari et al., 2007). This may be the reason for the relatively low Exch-P in this study sea area. Fe-P is P bound or encapsulated by metal oxides or hydroxides such as Al, Fe and Mn through physicochemical interactions (Ruttenberg, 1992), which is also a potentially bioavailable P, is easily dissolved and released into water under anoxic or partially reductive environment, and is the main existing form controlling dissolved P in water (Andrieux-Loyer et al., 2008; Liu et al., 2022).

In this study, the content and proportion of Fe-P in Tot-P were higher than the corresponding values of the Huanghe River, the Changjiang River and the Changjiang River Estuary (He et al., 2010; Meng et al., 2015), which could be related to the adsorption of part of active Org-P by iron and manganese oxides (Vink et al., 1997), or influenced by the high content of Fe-P (Wang et al., 2009) transported in the breeding area of Rushan Bay. The significant correlations between Fe-P and Fe_{CDB}, Fe-P and Mn_{CDB}

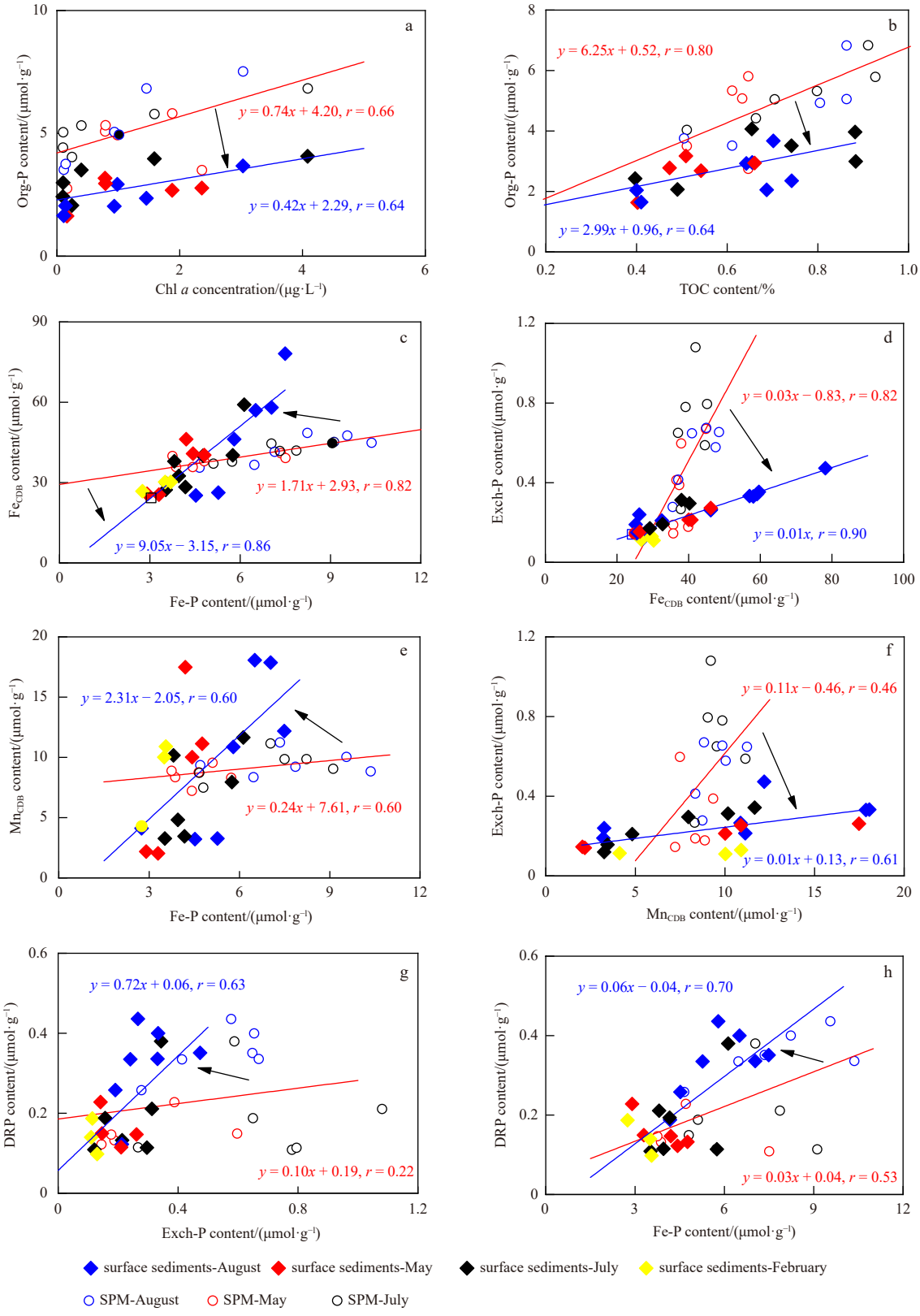

Fig. 2. Relationships between different forms of P and other parameters in water column, suspended particulate matter (SPM) and sediment. Exch-P: exchangeable phosphorus; Fe-P: iron-bound phosphorus; Org-P: organic P; TOC: total organic carbon; CDB: sodium citrate-dithionite-bicarbonate; DRP: dissolved reactive P.

(Figs 2c, e) indicate the control effect of active Fe-Mn oxide on active P (Zaaboub et al., 2014). In this study, there was a significant linear correlation between Exch-P and Fe-P ($r = 0.71$, $p < 0.01$, $n = 17$), reflecting the internal relationship between them. In fact, Fe-P and Exch-P are the most active particulate P in water environment (Andrieux-Loyer et al., 2008; Meng et al., 2014), and the

significant correlations between Fe_{CDB} and Exch-P, Mn_{CDB} and Exch-P (Figs 2d, f) also indicated the adsorption of active P by Fe and Mn oxides.

Auth-P is usually dominated by authigenic calcium carbonate fluorapatite (CFAP), bioapatite, and calcium carbonate P (Ca-P) (Ruttenberg, 1992; Jilbert and Slomp, 2013), which reflects the presence of P mainly from marine authigenic sources. The Auth-P has a slower kinetic formation rate, usually seen as "stable phosphorus" (Ruttenberg, 1992). Auth-P in SPM was mainly from biogenic apatite components in the Changjiang River Estuary (Meng et al., 2014) and Nazare Canyon (Van der Zee et al., 2002). Again, Auth-P in Rushan Bay were mainly from marine authigenic sources (Liu et al., 2016). Although Auth-P is generally not easily soluble, but it can be converted to dissolved phosphate when pH decreases or acidity increases (Adhikari et al., 2015; Liu et al., 2016). The percentage of Auth-P in Tot-P in the area off Rushan Bay was close to that in the Changjiang River Estuary SPM (9.6% ± 5.5%) (Meng et al., 2015), but lower than that in the Huanghe River (28%–50%) (He et al., 2010). This difference in Auth-P abundance was obviously related to the source of particulate matter. In the high-salinity estuary (such as the Changjiang River Estuary) and the coastal sea area (this study area), the proportion of terrigenous derived Ca-P decreases under the influence of seawater dilution (Zaaboub et al., 2014), thus reducing the proportion of Auth-P to Tot-P.

Det-P is mainly apatite of igneous and metamorphic rocks, which is generally not easy to decompose and can be used as an indicator of terrigenous input (Meng et al., 2015; Liu et al., 2020). The proportion of Det-P in Tot-P in the study area was the highest, and the content of Det-P in the SPM of the nearshore station was higher than that in the offshore area. Although the content of Det-P in the coastal waters of Rushan Bay is lower than that in the SPM of the Huanghe River, the Changjiang River and the adjacent waters of the Changjiang River Estuary, it still reflects the basic characteristics that particulate P is mainly imported from terrestrial sources.

Org-P contains biologically relevant active organic components such as orthophosphate monophosphate, polyphosphate or pyrophosphate (Lukkari et al., 2007; Cai and Guo, 2009; Lukkari et al., 2009), and P bound to inert organic matter such as humic or fulvic acids (Vink et al., 1997; Zhang et al., 2004). Usually Org-P can be used to indicate the impact of biological activities and primary production levels on natural water bodies (Zhang et al., 2004; Lin et al., 2013). In this study, the content of Org-P in particulate matter in water was linearly and positively correlated with the concentration of Chl *a* in water (Fig. 2a), reflecting the influence of primary production level on particulate Org-P.

4.2 *The form and distribution of P in sediments*

Bulk sediment digestions can give useful information on the fluxes and behaviour of P in marine environments (Defforey and Paytan, 2018; Liu et al., 2020). The concentration of Tot-P in the surface sediments in the study area was higher than that in the marginal seas of the eastern shelf of China, such as the Yellow Sea and Bohai Sea (7.5–20 μmol/g) (Liu et al., 2004) and the East China Sea ((17.5 ± 1.93) μmol/g) (Fang et al., 2007). However, the contribution of Exch-P to Tot-P was fairly low, accounting for only 1.4%. The content and relative proportion of Exch-P were lower than those in the Changjiang River Estuary (Meng et al., 2014) and close to those in the Yellow Sea and Bohai Sea (Liu et al., 2004). The content of Exch-P in sediments was positively correlated with the clay composition ($r = 0.80$, $p < 0.01$, $n = 9$), indicating that Exch-P could be easy to adsorb on the surface of fine particles. Fine particle size particles have a larger specific surface area than coarse particles, which is more conducive to the balance of reactive P components on the surface of particles (Andrieux-Loyer and Aminot, 2001; Meng et al., 2015). In addition, Fe_{CDB} and Mn_{CDB} were significantly correlated with Exch-P (Figs 2d, f), indicating the obvious adsorption of active P on Fe/Mn oxides, because Fe/Mn oxides or hydroxide colloids are easily adsorbed on the surface of fine particles and coprecipitate with Exch-P (Slomp et al., 1998; Andrieux-Loyer and Aminot, 2001), leading to the enrichment of Exch-P on fine particles.

Content and proportion of Fe-P in sediments of the coastal area off Rushan Bay were higher than those in the Changjiang River Estuary and the inland shelf of the East China Sea (Meng et al., 2014), the Yellow Sea and Bohai Sea, but significantly lower than those in the breeding area inside Rushan Bay (Wang et al., 2009; Table 4). Fe-P was positively correlated with Fe_{CDB} and Mn_{CDB} (Figs 2c, e), indicating that the content and activity of Fe and Mn oxides in sediments affected their ability to adsorb activated P. The content of Fe-P in sediments was positively correlated with the clay composition ($r = 0.79$, $p < 0.01$, $n = 9$) (Table S3). Like Exch-P, Fe-P is also easily adsorbed on the surface of fine particles, indicating that the grain size of sediment was also one of the factors controlling the occurrence of Fe-P.

The content and percentage of Auth-P in sediments are higher than those in the Yellow Sea, Bohai Sea and Changjiang River Estuary (Meng et al., 2014), and the corresponding values in the sediments of the East China Sea, and lower than those in the sediments of Rushan Bay (Wang et al., 2009). Auth-P in sediments of the East China Sea is mainly in the form of CFAP (Meng et al., 2014). Rushan Bay is an important economic shellfish culture area, and abundant shell debris can be observed in the sediment during sample processing. Obviously, the contribution of calcareous biological residues to sediment Auth-P may be an im-

Table 4. Summary of sediment type, P speciation and total organic carbon (TOC) in different coastal systems. P fractions are extracted with the chemical continuous extraction method

Site	Sediment type	Fe-P/ (μmol·g^{-1})	Auth-P/ (μmol·g^{-1})	Detr-P/ (μmol·g^{-1})	Org-P/ (μmol·g^{-1})	Tot-P/ (μmol·g^{-1})	TOC/%	Reference
Inner Rushan Bay (China)	clay	11.1 ± 0.9	13.0 ± 2.0	7.0 ± 1.0	6.1 ± 2.1	38.4 ± 6.2	0.8–1.2	Wang et al. (2009)
Rushan Bay (China)	clay	4.7 ± 1.4	2.1 ± 0.8	6.8 ± 1.6	2.94 ± 0.89	16.8 ± 1.61	0.4–0.9	this study
East China Sea	clay and silt	0.9–1.9	0.5–1.8	9.4–17	1.1–5.9	14–22	0.2–0.8	Fang et al. (2007); Hu et al. (2012)
Laizhou Bay (China)	clay	0.2–1.6	ND	7.4–13.2	0.7–2.9	10.2–18.8	ND	Zhuang et al. (2014)
Zhangzi Island (China)	clay	0.6–1.6	ND	0.5–6.6	0.7–2.8	2.6–12.9	ND	Zhuang et al. (2014)
Armação do Itapocoroy Bay (southern Brazil)	ND	0.02–0.12	0.6–1.6	0.02–0.09	0.02–0.18	5.7–9.4	ND	Souza et al. (2022)

Note: Fe-P: iron-bound phosphorus; Auth-P: authigenic P; Det-P: detrital-P; Org-P: organic P; Tot-P: total P; TOC: total organic carbon; ND: no available data.

portant reason for the higher content of Auth-P in the study area than in the eastern shelf sea of China. This finding also showed a similar phenomenon in the mariculture area of Laizhou Bay (Zhuang et al., 2014). Previous studies have found that the content of Ca-P, which is mainly produced by biological activities, can be up to about 20 μmol/g in the sediment of mussel culture area, which is the main component of Auth-P, accounting for 60%-80% of Tot-P (Zaaboub et al., 2014). It can be seen that mariculture activities have a significant impact on the distribution of P forms.

The content of Org-P in the offshore sediments off Rushan Bay is higher than that of the East China Sea, and close to that of the Yellow Sea, Bohai Sea and Changjiang River Estuary (Meng et al., 2014), lower than the sediment in Rushan Bay (Wang et al., 2009). The content of Org-P in sediments was positively correlated with TOC (Fig. 2b), and the content of Org-P was positively correlated with clay composition ($r = 0.81$, $p < 0.01$, $n = 9$). For organic matter, fine particles are also conducive to the preservation of organic matter, so the contents of TOC and Org-P are relatively high in some muddy areas (Meng et al., 2014). The correlation between Org-P and TOC, fine particle fraction, and Chl *a* in sediments also reflects that the distribution of Org-P was jointly controlled by hydrodynamic forces on sediment sorting and distribution of primary productivity (Fig. 2).

The content of Det-P and its percentage in Tot-P in the offshore sediments of Rushan Bay were significantly lower than those in the tidal flat wetlands of the Changjiang River Estuary and the East China Sea (Hou et al., 2009). It is close to the Yellow Sea and Bohai Sea (Liu et al., 2004), but also lower than the sediment of shellfish farms in Rushan Bay (Wang et al., 2009). There was a significant negative correlation between Det-P content and clay composition ($r = 0.80$, $p < 0.01$, $n = 9$), but positively correlated with sand content ($r = 0.63$, $p < 0.01$, $n = 9$), suggesting the Det-P should mainly come from the products of soil or rock weathering and erosion which was exported by surface runoff. The terrestrial contribution of particle is also the main reason for the high content and relative proportion of Det-P in the East China Sea (Table 4). However, in the far-reaching sea, the terrestrial input is relatively small, and Det-P is the existing form with relatively small contribution to P in sediments (Schenau et al., 2005).

4.3 *P transformation in water, particulate matter and sediment*

The concentrations of each P form and the percentage of Tot-P in SPM in coastal waters off Rushan Bay have different characteristics. The dynamic partitioning of P among dissolved and particulate phases should play a critical role in controlling the abundance, transformation, bioavailability, and the overall biogeochemical cycling of P in aquatic environments (Meng et al., 2015; Liu et al., 2016). There is a strong interconversion between dissolved P and particulate P, especially in the brackish and freshwater mixed estuarine region and in the hypoxic offshore environment (Lin et al., 2013, 2016; Leote and Epping, 2015). The adsorption and desorption process of P on SPM surface is affected by particle size, salinity and temperature, and is also related to the competitive adsorption of anions (Cl^-, SO_4^{2-}, HCO_3^-, OH^- and Br^-), the DIP level of water and the equilibrium concentration of P adsorption (Millero et al., 2001). There was a significant positive correlation between the active exchangeable P (Exch-P and Fe-P) in DRP and SPM in the study area, which reflects the dynamic chemical equilibrium between DIP and particulate active inorganic P (Eq. (1)).

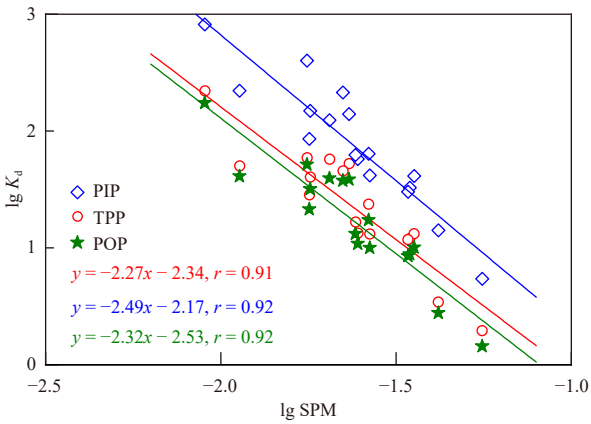

Fig. 3. Relationship between partition coefficient (lg K_d) of P and suspended particulate matter concentration (in lg SPM) in this study. PIP: particulate inorganic P; POP: particulate organic P; TPP: total particulate P.

The relationship between the partition coefficient lg K_d and SPM shows that the lg K_d of inorganic P and Org-P decreases with the concentration of SPM (Fig. 3). Many elements with reactivity with particulate matter have similar phenomena in the water environment (Lin et al., 2016). The lg K_d values of inorganic P and Org-P were significantly correlated with SPM ($p < 0.001$), indicating that both of them have certain particle activity, which is also the reason why active particulate P (Exch-P, Fe-P and Org-P) is more likely to combine with fine particles. For Org-P, biological processes and microbial degradation may be the main factors affecting Org-P partitioning, which is also reflected in the relationship between particulate Org-P and Chl *a*, Org-P and particulate organic carbon (Figs 2a, b). In addition, the similarity between the partition coefficient of Org-P and inorganic P is also a prerequisite for Org-P to be used and transformed by organisms, which is of great significance in natural water bodies where reactive phosphate is a limiting source element (Duhamel et al., 2021). Therefore, the surface area of colloid and particulate matter, phytoplankton cells, and particle-particle exchange processes (such as flocculation and co-precipitation) would all affect the distribution coefficient of P, so as to change or regulate the concentration of DIP in water (Duhamel et al., 2021).

Another mechanism of dissolved P from aqueous phase to solid phase in the aquatic environment is co-precipitation with calcium carbonate or adsorption by ferric manganese oxide colloidal. Before permanent burial, P generally goes through several release-deposit-re-release-re-deposition processes, and finally only a small part of P is preserved in the sediment (Schenau et al., 2005). In this study, during particles settling into surface sediments, all forms of P had changed to different degrees (Fig. 4). From SPM to sediment, the content of Tot-P decreased by 23%, Exch-P decreased by 56%, Fe-P decreased by 28%, Org-P decreased by 42%, and bioavailable P decreased by 35%, while Auth-P and Det-P changed slightly (~1%). This means approximately 23% of P in SPM had been released in the water column before the SPM settled to the sediment. The proportion of each P form to Tot-P in sediments and SPM were also different. Compared with SPM, ratio of Exch-P/Tot-P in sediments was reduced by 43%, Fe-P/Tot-P by 6%, Org-P/Tot-P by 24%, and bioavailable P to Tot-P by 15%, respectively. As a result, Auth-P and Det-P were increased by 31% and 15%, respectively.

Auth-P has a slow formation rate and is the final product of

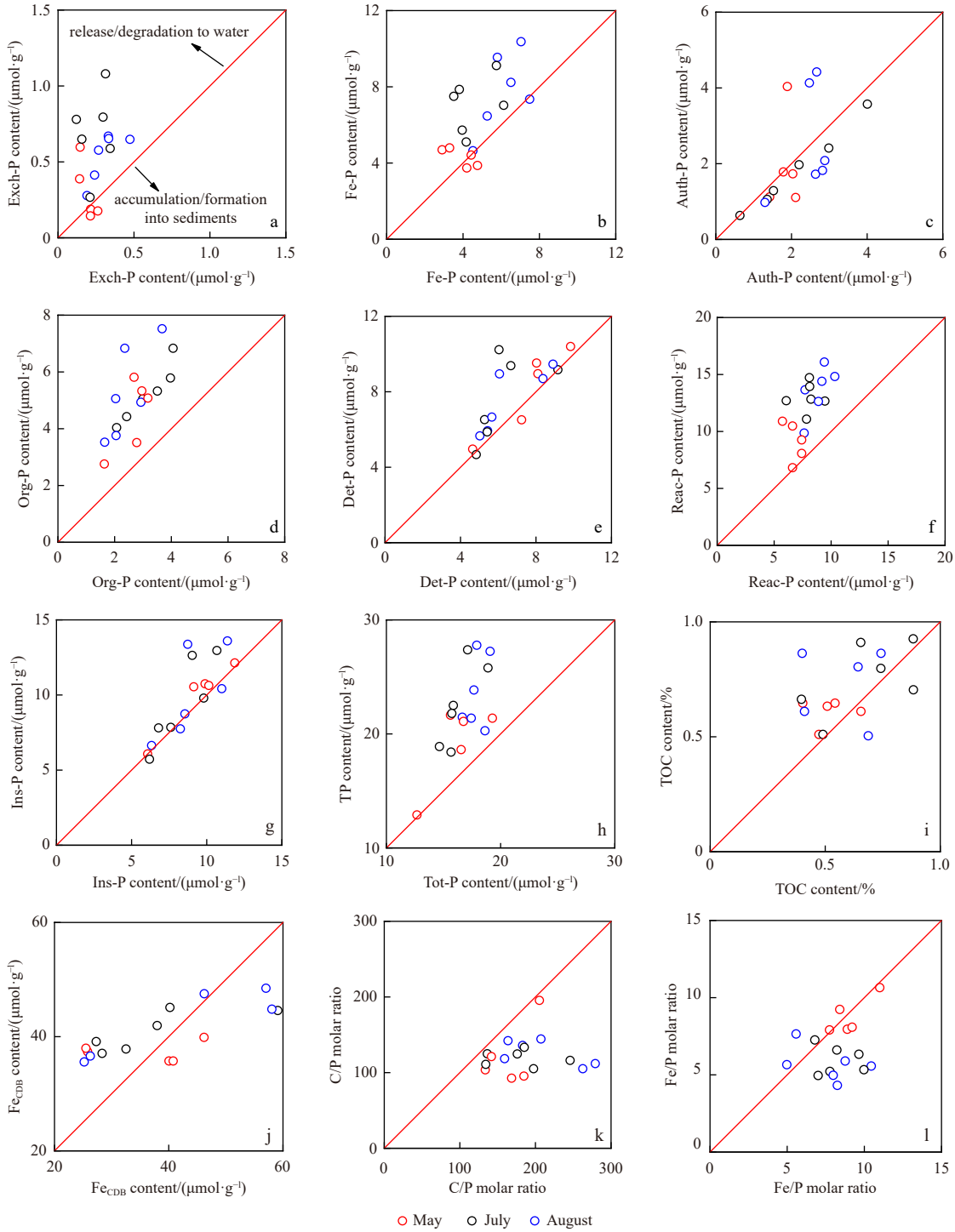

Fig. 4. Contents of different P forms in suspended particulate matter (SPM) and sediment (Ins-P, is difficult to decompose, namely, the sum of authigenic P (Auth-P) and detrital-P (Det-P); the horizontal axis is sediment content, and the vertical axis is SPM content. The data points located in >1:1 region represents the release/degradation during the deposition process, and the data located in <1:1 area indicate enrichment/generation occurring during the deposition process). Exch-P: exchangeable phosphorus; Fe-P: iron-bound phosphorus; Reac-P: reactive phosphorus; Org-P: organic P; Tot-P: total P; TOC: total organic carbon; CDB: sodium citrate-dithionite-bicarbonate; C/P molar ratio: molar ratio of Org-P and TOC.

diagenesis after active P deposition and burial, while Det-P is generally an inert component, so Auth-P and Det-P belong to the category of P that cannot be reused or difficult to be utilized normally. In the early diagenetic process of suboxidation, the mineralization of sedimentary organic carbon will also accelerate the formation of authigenic minerals (Yao et al., 2014; Liu et al., 2020). The hypoxic environment and aquaculture activities in Rushan Bay are likely to cause the rapid formation of autogenous calcium-fluorapatite (Zaaboub et al., 2014; Zhuang et al., 2014) and accumulate in the sediments. However, Auth-P phases in

sediments also include P associated with Fe-oxides, which eventually forms Auth-P (Jilbert and Slomp, 2013). This process could also explain the small Auth-P loss in SPM during deposition from water column to sediment (Fig. 4c). Again, the iterative resuspension of sediment may drive the phosphorus speciation redistribution by the thinning process (Liu et al., 2016), leading to the content of Det-P lower (Fig. 4e).

The difference of Exch-P in particulate matter and sediment further proves that Exch-P, as an active form of P, has a higher conversion rate than other occurring forms of P. The content of Exch-P in sediments reflects its dynamic equilibrium state of adsorption-desorption on mineral surface. The main carriers of Exch-P in sediments are metal oxides or hydroxides and other fine particles (Andrieux-Loyer and Aminot, 2001; Zhuang et al., 2014), in addition, hydrodynamic conditions, biological disturbance and redox conditions are also important factors affecting Exch-P migration. In particular, during the migration of particulate matter from water to sediment, the partially reductive sediment is conducive to the desorption of Exch-P, which is also an important reason for the significant correlation between DRP and Exch-P content in the overlying water (Fig. 2g). Similar to Exch-P, Fe-P was partially lost during migration from particulate matter to sediment. CDB solution mainly extracted P bound to weak crystalline and amorphous iron oxides (Ruttenberg, 1992), although there was a significant linear correlation between Fe-P and Fe_{CDB} in both SPM and sediment (Fig. 2c), the Fe/P ratio decreased from 11 in SPM to 8 in sediment, and the Fe_{CDB} content in SPM and sediment did not change significantly. Apparently, the more reductive environment promotes the dissolution and release of Fe-P (Noffke et al., 2012). Usually, Fe/P ratios between 2 and 20 can be regarded as P released mainly from the reduction and dissolution of active Fe-P (Slomp et al., 1996; Noffke et al., 2012). In this study, Fe/P was averaged 2, and there was a significant correlation between DRP and Fe^{2+} in the overlying water ($r = 0.66$, $p < 0.01$, $n = 20$), and DRP and Fe-P in sediments (Fig. 2h). Obviously, part of DRP in the overlying water was derived from the dissolution and release of Fe-P in sediments, while Fe^{2+} was reoxidized and stored in the surface of sediments.

The content of Fe-P was influenced both by source and transformation. First, Fe^{2+} in water column in surface layer was higher in February and May (high DO concentration), but lower in July and August (low DO concentration), which created the different oxidation-reduction conditions for high or low Fe-P formation. Second, the difference of Fe-P content between SPM and sediment decreased with the increasing of overlying water DO (Fig. 5). These means the released DRP from Fe-P also decreases with the increasing of overlying water DO.

4.4 *Benthic processes of P in water-sediment system*

Phosphate release from particulate organic matter (POM) dominates P cycling in aquatic ecosystems (Guo et al., 2023). The degradation of Org-P in the sediments and SPM was evident from the relationship between Org-P and TOC and the change of C/P molar ratio (Figs 2b, 4k). In SPM, C/P ratio varied from 92 to 195 with an average of 122 ± 24, which was slightly higher than the Redfield ratio of phytoplankton (106:1). Since different types of organic matter have different molar ratios of TOC to TON (C/N), C/N in sediments, which can be used to roughly distinguish the sources of organic matter in sediments. Generally, the C/N ratio of soil organic matter is about 8–15, that of marine organic matter is less than 8, and that of terrestrial plants is more than 15. Also, C/N ratio associated with organic matter is affected by hydrological conditions and biological effects (Kendall et al., 2001). The $\delta^{13}C$ value of terrestrial C3 plants ranges from –32‰ to –22‰, and that of C4 plants ranges from –16‰ to –9‰ (Kendall et al., 2001). The $\delta^{13}C$ value of soil organic matter ranges from –22‰ to –25‰; and that of riverine plankton and aquatic plants ranged from –24‰ to –42‰ and –18‰ to –28‰, respectively (Lu et al., 2013). In this study, the ratio of C/N in SPM was 6 ± 1, and $\delta^{13}C$ ranged from –22.1‰ to –20.4‰, indicating that organic carbon was mainly derived from algae. According to the end-member model calculation of organic carbon provenance, $\delta^{13}C_M$ (–19.5‰) and $\delta^{13}C_T$ (–27‰) are the $\delta^{13}C$ values of material with marine and terrestrial origins, respectively (Wu et al., 1999), the results show that marine organic carbon accounted for 65%–88%, while terrestrial organic carbon contributed to a smaller proportion (25%), indicating that Org-P in the offshore SPM of Rushan Bay was also mainly derived from marine organisms. From SPM to sediment, TOC content decreased by 17%, while Org-P decreased by 42%, indicating that Org-P degradation rate was faster than that of SPM. The C/P ratio in sediments ranged from 130 to 280, with an average value of 190 ± 44, which was significantly higher than Redfield ratio and that in SPM, indicating that the organic matter was degraded in the early diagenetic stage during the deposition of particulate matter. In addition, autogenetic marine TOC is generally more easily degraded than terrestrial TOC (Goñi et al., 1997; Muller-Karger et al., 2005), which is also the reason for such a difference composition in Org-P in SPM and sediment.

4.5 *Influence of DO on the P transformation in aquaculture area*

Sediments overlain by oxygenated water column often bear large amounts of P bound to Fe and Mn oxides (Defforey and Paytan, 2018), while sediments overlain by hypoxic bottom water are more depleted in these phases and often harbor more P bound to calcium mineral (Kraal et al., 2017; Liu et al., 2020). To some extent, hypoxia can promote the release of P from SPM and sediments into the water column (Reed et al., 2011), this part of P mainly comes from the transformation of Exch-P and Fe-P (Zhang et al., 2012; Adhikari et al., 2015), which also explains why the Fe/P value under low DO condition is lower than that under oxygen-rich condition. The relationship between DO and DRP, Exch-P and Fe-P in the overlying water (Figs 2g, h and 5a) also revealed that low DO level accelerated the regeneration of inorganic P in SPM and surface sediments, which is also found in some low DO water bodies (Reed et al., 2011; Liu et al., 2020).

Generally, both organic matter degradation and Fe/Mn oxides dissolution can increase DRP in the column. The differences of P forms in SPM and sediment (Fig. 4), and the sediment incubation implemented in Rushan Bay (Liu et al., 2016), actually showed that Fe-P dissolution under low DO condition was the main process to increase DRP. In addition, iron manganese oxide, calcium carbonate bound P and other Auth-P in SPM also tend to dissolve under low oxygen conditions (Lin et al., 2016; Liu et al., 2020), becoming the main source of P in the water column. The reduction of iron oxides dominates the release of P in both freshwater and seawater particulate matter (Slomp et al., 1996; Liu et al., 2020). In the partial oxidation environment, the Fe/P ratio can decrease to $\ll 1$ in sediments (Noffke et al., 2012), which may be that the dissolved Fe^{2+} is then adsorbed and reoxidized by particulate matter and removed from the water body (Noffke et al., 2012). The low ratio of Fe^{2+} and DRP in the water outside Rushan Bay (0.04–0.20) also reflects the role of oxygen in controlling P abundance.

In this study, when DO was high (DO > 250 μmol/L), the C/P ratio values in sediments and SPM were fairly low, especially the

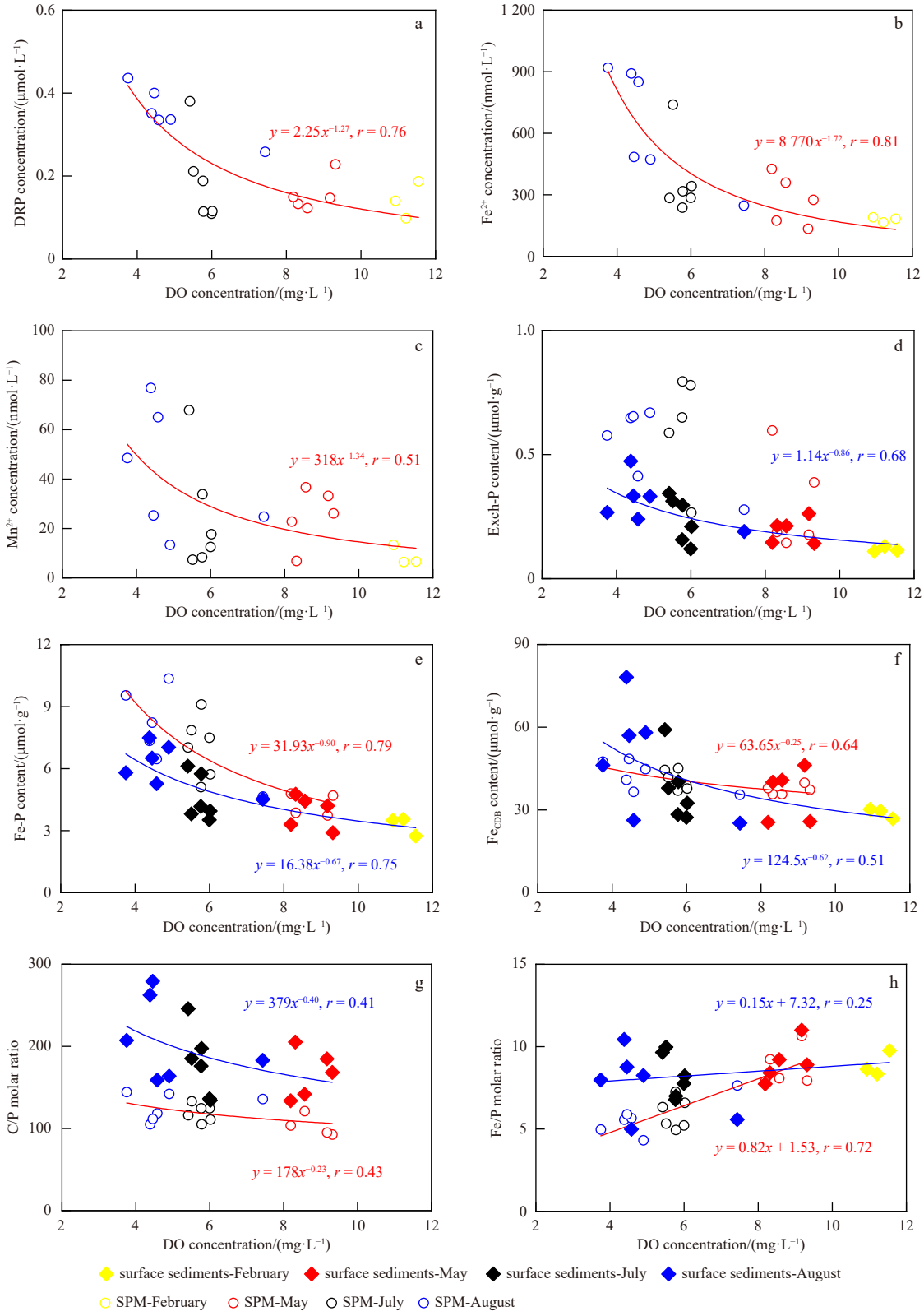

Fig. 5. Relationships between overlying water DO and fractionations of P, Fe and Mn in the overlying water suspended particulate matter (SPM) and surface sediments. Exch-P: exchangeable phosphorus; Fe-P: iron-bound phosphorus; DRP: dissolved reactive P; CDB: sodium citrate-dithionite-bicarbonate; C/P molar ratio: molar ratio of total organic C and organic P.

C/P value in SPM was close to Redfield ratio (Table 2). However, in the case of low DO (DO < 160 μmol/L), there was a high C/P value of SPM (Fig. 5g). The above results showed that there was significant degradation of organic carbon in water with high DO content, and the conservation efficiency of TOC in low-DO water was higher than that in oxygen-rich water (McKee et al., 2004).

However, in low-DO environment, Org-P was preferentially recycled and recycled into water. Therefore, the preservation efficiency of Org-P is also controlled by the level of DO, which is significantly different from that of TOC. The relationship between hypoxia and Org-P kinetics and the degradation degree of TOC can be realized by the C/P ratio. It can be seen that hypoxia changes the distribution and morphological composition of various forms of P in SPM and sediment, and then affects the content and source of phosphate in water, making sediment shift from a sink to a source of P in marine water. P recycling in hypoxic water also has a positive feedback to eutrophication, especially in the water with high P limitation. On the other hand, the supplement of DIP will also promote the flourishing of phytoplankton, and the new organic particulate matter will increase the consumption of DO in water, and create material conditions for the formation, maintenance and even deterioration of hypoxia (Adhikari et al., 2015). In this study, the N/P ratio of DIN and DRP in water ranged from 8 to 81, with an average value of 23, which was higher than Redfield ratio, indicating a potential P limitation. However, the occurrence of hypoxia is likely to promote the release of reactive P and lead to the increase of water DRP (Fig. 5a), which alleviates the P limitation in water. The release of P may induce the bloom of algae and further aggravate the hypoxia condition, which has been recorded in many hypoxia seas (Rozan et al., 2002; Adhikari et al., 2015).

In fact, the exchange rate of Exch-P and Fe-P at the solid-liquid interface is very fast. Adhikari et al (2015) found that the release rate of P is positively and significantly correlated with the content of Fe-P in the sediments of Gulf of Mexico. The P released after 30 d accounted for 0.1%–6.9% of the Tot-P, while Fe-P accounted for 0.5%–10% of the Tot-P, indicating that Fe-P had quite high solubility activity (Adhikari et al., 2015). The results of culture experiments in the sediment of Rushan Bay under different DO conditions show that iron and manganese oxides are dissolved and released to a certain extent under oxygen-rich, hypoxic and anoxic conditions, and the release rate and amount increase with the decrease of DO. In addition, under the condition of 63 μmol/L DO for 15 d, almost all of the released P, iron and manganese were derived from CDB extracts, while no iron and manganese release behavior was observed under oxygen-rich conditions (Liu et al., 2022). In this study, sediments were incubated continuously for 20 d at a DO of 100–150 μmol/L, and about 48% of the Fe-P in sediments was released into the overlying water (Liu et al., 2016). Based on the sediment incubation implemented of the Rushan Bay (Liu et al., 2016) and Changjiang River Estuary (Liu et al., 2020), Fe-P dissolution under low DO condition was the main process to increase DRP in the overlying water. It can be seen that SPM and sediments in the study area have a great potential for P release, especially under seasonal low oxygen conditions, and Exch-P and Fe-P could be likely to be released into the water body and re-change the structure of water nutrients.

Combined with this study and related culture experiments (Adhikari et al., 2015; Liu et al., 2022), assuming that under the secondary oxidation condition (DO: 100–150 μmol/L), about 50% of Exch-P and Fe-P in the particulate matter and surface sediment (thickness 1 cm) could be released into the water. Under the absence of oxygen in the overlying water, Exch-P and Fe-P tend to release into the water through the transformation process. Under the condition of rich oxygen (DO > 260 μmol/L), the dissolved release of P was almost none. With DRP, DIN, Exch-P and Fe-P as the background (DO > 260 μmol/L), without considering the changes of water exchange and DIN, the concentration

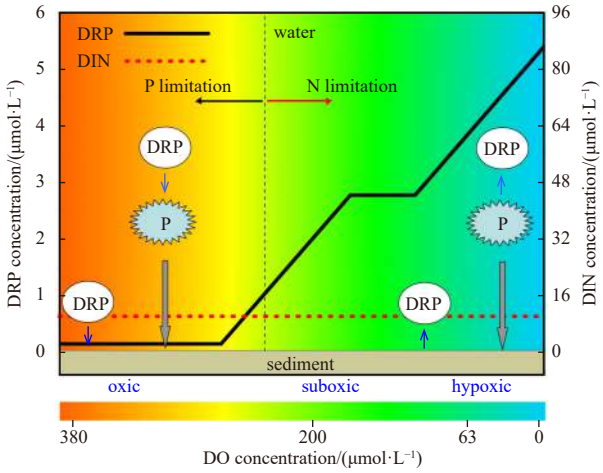

Fig. 6. A conceptual model showing the influence of DO on the potential dissolved reactive P (DRP) release in the water column. DIN: dissolved inorganic nitrogen.

of SPM and the density of sediment (1.5 g/cm^3) were combined to calculate the concentration of DRP and nutrient structure level in water under different DO conditions (Fig. 6). It can be seen that under oxygen-rich conditions, as water DRP:DIN was less than 16:1, P become a potential limiting element. While, when the water body developed to the hypoxic state, the P limitation was obviously improved. When the water body was in a state of low oxygen, a large amount of reactive P released from SPM and sediment, which would greatly increase the concentration of DRP in the water body, thereby resulting in the deterioration of water quality (Rozan et al., 2002; Adhikari et al., 2015). Despite the extreme low oxygen environment in the coastal area off Rushan Bay are less likely to occur, but in recent years, with the intensification of human activity factors, the mariculture site could cause seasonal hypoxia and face further eutrophication risk (Liu et al., 2016; Zhang et al., 2022), which would be also the common concern of many mariculture areas with anoxic waters at present and deserves further attention.

5 Conclusions and future directions

The content, form and seasonal distribution of P in SPM and sediment were significantly different in the coastal area off Rushan Bay due to the differentiation transformation process, different sources and influence of mariculture. Det-P and Fe-P were the main forms of P in both SPM and surface sediments in the coastal area off Rushan Bay. Exch-P and Fe-P were largely controlled by Fe and Mn oxides and particle size, while Org-P was mainly related to primary production. The partition coefficient of P showed that both particulate inorganic P and Org-P had high reactivity, indicating that the regeneration of particulate P, utilization and transformation by organisms were key controlling processes of P in water.

During the deposition of SPM from the water column to the sediment, the occurrence forms of P changed, and the contents of Exch-P, Fe-P and Org-P and their contributions to Tot-P decreased significantly. The relationships between water DO and DRP, Exch-P and Fe-P suggested that low DO level accelerated the regeneration of inorganic P in SPM and surface sediments. Under seasonal hypoxia conditions, the effect of DO on the potential release of DRP showed that Exch-P and Fe-P in sediment released into the water column through transformation would increase the risk of eutrophication.

Mariculture could enhance the deoxygenation in the water column due to the degeneration of organic carbon, which would alter the P cycling in the water-sediment system. It is advisable to predict and explain the changing characteristics of P cycling under the increasing pressure from mariculture at present and in the future.

Acknowledgements

We would like to express our deep gratitude to our colleagues for their assistance on board and laboratory work. Insightful comments and suggestions from two anonymous reviewers have greatly improved this work.

References

Adhikari P L, White J R, Maiti K, et al. 2015. Phosphorus speciation and sedimentary phosphorus release from the Gulf of Mexico sediments: Implication for hypoxia. Estuarine, Coastal and Shelf Science, 164: 77–85

Andrieux-Loyer F, Aminot A. 2001. Phosphorus forms related to sediment grain size and geochemical characteristics in French coastal areas. Estuarine, Coastal and Shelf Science, 52(5): 617–629

Andrieux-Loyer F, Philippon X, Bally G, et al. 2008. Phosphorus dynamics and bioavailability in sediments of the Penzé Estuary (NW France): in relation to annual P-fluxes and occurrences of *Alexandrium Minutum*. Biogeochemistry, 88(3): 213–231, doi: 10.1007/s10533-008-9199-2

Asmala Eero, Carstensen Jacob, Conley Daniel J, et al. 2017. Efficiency of the coastal filter: Nitrogen and phosphorus removal in the Baltic Sea. Limnology and Oceanography, 62(S1): 222–238

Ballagh A E F, Rabouille C, Andrieux-Loyer F, et al. 2021. Spatial variability of organic matter and phosphorus cycling in Rhône River prodelta sediments (NW Mediterranean Sea, France): a model-data approach. Estuaries and Coasts, 44: 1765–1789

Cai Yihua, Guo Laodong. 2009. Abundance and variation of colloidal organic phosphorus in riverine, estuarine, and coastal waters in the northern Gulf of Mexico. Limnology and Oceanography, 54(4): 1393–1402, doi: 10.4319/lo.2009.54.4.1393

Defforey D, Paytan A. 2018. Phosphorus cycling in marine sediments: Advances and challenges. Chemical Geology, 477: 1–11, doi: 10.1016/j.chemgeo.2017.12.002

Dong Xumeng, Ma Shuonan, Wang Haijun, et al. 2022. Dissolved organic carbon loading stimulates sediment phosphorus mobilization and release: preliminary evidence from Xiangshan Port, East China Sea. Frontiers in Environmental Science, 9: 782701, doi: 10.3389/fenvs.2021.782701

Duhamel S, Diaz J M, Adams J C, et al. 2021. Phosphorus as an integral component of global marine biogeochemistry. Nature Geoscience, 14(6): 359–368, doi: 10.1038/s41561-021-00755-8

Fang Tien-Hsi, Chen Jui-Lin, Huh Chih-An. 2007. Sedimentary phosphorus species and sedimentation flux in the East China Sea. Continental Shelf Research, 27(10–11): 1465–1476, doi: 10.1016/j.csr.2007.01.011

Go Y S, Kim C S, Lee W C, et al. 2023. A stable isotopic approach for quantifying aquaculture-derived organic matter deposition dynamics in the sediment of a coastal fish farm. Marine Pollution Bulletin, 192: 115132, doi: 10.1016/j.marpolbul.2023.115132

Goñi M A, Ruttenberg K C, Eglinton T I. 1997. Sources and contribution of terrigenous organic carbon to surface sediments in the Gulf of Mexico. Nature, 389(6648): 275–278, doi: 10.1038/38477

Guo Minli, Li Xiaolu, Wang Yi, et al. 2023. New insights into the mechanism of phosphate release during particulate organic matter photodegradation based on optical and molecular signatures. Water Research, 236: 119954, doi: 10.1016/j.watres.2023.119954

He Huijun, Yu Zhigang, Yao Qingzheng, et al. 2010. The hydrological regime and particulate size control phosphorus form in the suspended solid fraction in the dammed Huanghe (Yellow River). Hydrobiologia, 638(1): 203–211, doi: 10.1007/s10750-009-0041-1

He Hui, Zhen Yu, Mi Tiezhu, et al. 2017. Measurement of potential nitrification rates in sediments from adjacent waters of Rushan Bay. China Environmental Science (in Chinese), 37(3): 1082–1088

Hou Lijun, Liu Min, Yang Yi, et al. 2009. Phosphorus speciation and availability in intertidal sediments of the Yangtze Estuary, China. Applied Geochemistry, 24(1): 120–128, doi: 10.1016/j.apgeochem.2008.11.008

Hu Limin, Shi Xuefa, Yu Zhigang, et al. 2012. Distribution of sedimentary organic matter in estuarine-inner shelf regions of the East China Sea: Implications for hydrodynamic forces and anthropogenic impact. Marine Chemistry, 142–144: 29–40

Islam S. 2005. Nitrogen and phosphorus budget in coastal and marine cage aquaculture and impacts of effluent loading on ecosystem: review and analysis towards model development. Marine Pollution Bulletin, 50(1): 48–61, doi: 10.1016/j.marpolbul.2004.08.008

Jilbert T, Slomp C P. 2013. Iron and manganese shuttles control the formation of authigenic phosphorus minerals in the euxinic basins of the Baltic Sea. Geochimica et Cosmochimica Acta, 107: 155–169, doi: 10.1016/j.gca.2013.01.005

Kendall C, Silva S R, Kelly V J. 2001. Carbon and nitrogen isotopic compositions of particulate organic matter in four large river systems across the United States. Hydrological Processes, 15(7): 1301–1346, doi: 10.1002/hyp.216

Kraal P, Dijkstra N, Behrends T, et al. 2017. Phosphorus burial in sediments of the sulfidic deep Black Sea: Key roles for adsorption by calcium carbonate and apatite authigenesis. Geochimica et Cosmochimica Acta, 204: 140–158

Leote C, Epping E H G. 2015. Sediment–water exchange of nutrients in the Marsdiep basin, western Wadden Sea: Phosphorus limitation induced by a controlled release?. Continental Shelf Research, 92: 44–58, doi: 10.1016/j.csr.2014.11.007

Lin Peng, Guo Laodong, Chen Min, et al. 2013. Distribution, partitioning and mixing behavior of phosphorus species in the Jiulong River Estuary. Marine Chemistry, 157: 93–105, doi: 10.1016/j.marchem.2013.09.002

Lin Peng, Klump J V, Guo Laodong. 2016. Dynamics of dissolved and particulate phosphorus influenced by seasonal hypoxia in Green Bay, Lake Michigan. Science of the Total Environment, 541: 1070–1082, doi: 10.1016/j.scitotenv.2015.09.118

Liu Jun, Krom M D, Ran Xiangbin, et al. 2020. Sedimentary phosphorus cycling and budget in the seasonally hypoxic coastal area of Changjiang Estuary. Science of the Total Environment, 713: 136389, doi: 10.1016/j.scitotenv.2019.136389

Liu Xiaotian, Liu Jun, Wang Yibin, et al. 2022. Phosphorus cycling in a sediment-water system controlled by different dissolved oxygen levels of overlying water. Environmental Science (in Chinese), 43(12): 5571–5584

Liu Jun, Zang Jiaye, Zhao Chenying, et al. 2016. Phosphorus speciation, transformation, and preservation in the coastal area of Rushan Bay. Science of the Total Environment, 565: 258–270, doi: 10.1016/j.scitotenv.2016.04.177

Liu Sumei, Zhang Jing, Li Daoji. 2004. Phosphorus cycling in sediments of the Bohai and Yellow Seas. Estuarine, Coastal and Shelf Science, 59(2): 209–218

Liu Ying, Zhang Xuechao, Li Xiaomin, et al. 2015. Profile characteristics of COD and its influencing factors in Rushan Bay and adjacent area. Fisheries Science (in Chinese), 34(10): 657–661

Lu Fengyun, Liu Zhuqing, Ji Hongbing. 2013. Carbon and nitrogen isotopes analysis and sources of organic matter in the upper reaches of the Chaobai River near Beijing, China. Science China: Earth Sciences, 56(2): 217–227, doi: 10.1007/s11430-012-4525-x

Lukkari K, Hartikainen H, Leivuori M. 2007. Fractionation of sediment phosphorus revisited. I: Fractionation steps and their biogeochemical basis. Limnology and Oceanography: Methods, 5(12): 433–444, doi: 10.4319/lom.2007.5.433

Lukkari K, Leivuori M, Kotilainen A. 2009. The chemical character and behaviour of phosphorus in poorly oxygenated sediments from open sea to Organic-Rich Inner Bay in the Baltic Sea.

Biogeochemistry, 96(1–3): 25–48, doi: 10.1007/s10533-009-9343-7
McKee B A, Aller R C, Allison M A, et al. 2004. Transport and transformation of dissolved and particulate materials on continental margins influenced by major rivers: benthic boundary layer and seabed processes. Continental Shelf Research, 24(7–8): 899–926, doi: 10.1016/j.csr.2004.02.009
Meng Jia, Yao Peng, Bianchi T S, et al. 2015. Detrital phosphorus as a proxy of flooding events in the Changjiang River Basin. Science of the Total Environment, 517: 22–30, doi: 10.1016/j.scitotenv.2015.02.053
Meng Jia, Yao Peng, Yu Zhigang, et al. 2014. Speciation, bioavailability and preservation of phosphorus in surface sediments of the Changjiang Estuary and adjacent East China Sea inner shelf. Estuarine, Coastal and Shelf Science, 144: 27–38
Millero F, Huang Fen, Zhu Xiaorong, et al. 2001. Adsorption and desorption of phosphate on calcite and aragonite in seawater. Aquatic Geochemistry, 7(1): 33–56, doi: 10.1023/A:1011344117092
Mort H P, Slomp C P, Gustafsson B G, et al. 2010. Phosphorus recycling and burial in Baltic Sea sediments with contrasting redox conditions. Geochimica et Cosmochimica Acta, 74(4): 1350–1362, doi: 10.1016/j.gca.2009.11.016
Muller-Karger F E, Varela R, Thunell R, et al. 2005. The importance of continental margins in the global carbon cycle. Geophysical Research Letters, 32(1): L01602
Noffke A, Hensen C, Sommer S, et al. 2012. Benthic iron and phosphorus fluxes across the Peruvian oxygen minimum zone. Limnology and Oceanography, 57(3): 851–867, doi: 10.4319/lo.2012.57.3.0851
Poulton S W, Canfield D E. 2005. Development of a sequential extraction procedure for iron: implications for iron partitioning in continentally derived particulates. Chemical Geology, 214(3–4): 209–221, doi: 10.1016/j.chemgeo.2004.09.003
Reed D C, Slomp C P, Gustafsson B G. 2011. Sedimentary phosphorus dynamics and the evolution of bottom-water hypoxia: A coupled benthic-pelagic model of a coastal system. Limnology and Oceanography, 56(3): 1075–1092, doi: 10.4319/lo.2011.56.3.1075
Rozan T F, Taillefert M, Trouwborst R E, et al. 2002. Iron-sulfur-phosphorus cycling in the sediments of a shallow coastal bay: Implications for sediment nutrient release and benthic macroalgal blooms. Limnology and Oceanography, 47(5): 1346–1354, doi: 10.4319/lo.2002.47.5.1346
Ruttenberg K C. 1992. Development of a sequential extraction method for different forms of phosphorus in marine sediments. Limnology and Oceanography, 37(7): 1460–1482, doi: 10.4319/lo.1992.37.7.1460
Schenau S J, Reichart G J, De Lange G J. 2005. Phosphorus burial as a function of paleoproductivity and redox conditions in Arabian Sea sediments. Geochimica et Cosmochimica Acta, 69(4): 919–931, doi: 10.1016/j.gca.2004.05.044
Slomp C P, Epping E H G, Helder W, et al. 1996. A key role for iron-bound phosphorus in authigenic apatite formation in North Atlantic continental platform sediments. Journal of Marine Research, 54(6): 1179–1205, doi: 10.1357/0022240963213745
Slomp C P, Malschaert J F P, Van Raaphorst W. 1998. The role of adsorption in sediment-water exchange of phosphate in North Sea continental margin sediments. Limnology and Oceanography, 43(5): 832–846, doi: 10.4319/lo.1998.43.5.0832
Souza G K, Kuroshima K N, Abreu J G N, et al. 2022. Speciation and distribution of sedimentary phosphorus in an important mariculture area, Armação do Itapocoroy Bay, Southern Brazil. Regional Studies in Marine Science, 49: 102137, doi: 10.1016/j.rsma.2021.102137
Van der Zee C, Slomp C P, Van Raaphorst W. 2002. Authigenic P formation and reactive P burial in sediments of the Nazaré canyon on the Iberian margin (NE Atlantic). Marine Geology, 185(3–4): 379–392, doi: 10.1016/S0025-3227(02)00189-5
Vink S, Chambers R M, Smith S V. 1997. Distribution of phosphorus in sediments from Tomales Bay, California. Marine Geology, 139(1–4): 157–179, doi: 10.1016/S0025-3227(96)00109-0
Wang Didi, Sun Yao, Shi Xiaoyong, et al. 2009. Distribution of nitrogen in sediments of eastern Rushan Bay. Marine Environmental Science (in Chinese), 28(6): 639–642
Wu Jinping, Calvert S E, Wong C S. 1999. Carbon and nitrogen isotope ratios in sedimenting particulate organic matter at an upwelling site off Vancouver Island. Estuarine, Coastal and Shelf Science, 48(2): 193–203
Yao Peng, Zhao Bin, Bianchi T S, et al. 2014. Remineralization of sedimentary organic carbon in mud deposits of the Changjiang Estuary and adjacent shelf: Implications for carbon preservation and authigenic mineral formation. Continental Shelf Research, 91: 1–11, doi: 10.1016/j.csr.2014.08.010
Zaaboub N, Ounis A, Helali M A, et al. 2014. Phosphorus speciation in sediments and assessment of nutrient exchange at the water-sediment interface in a Mediterranean lagoon: Implications for management and restoration. Ecological Engineering, 73: 115–125, doi: 10.1016/j.ecoleng.2014.09.017
Zhang Jiazhong, Fischer C J, Ortner P B. 2004. Potential availability of sedimentary phosphorus to sediment resuspension in Florida Bay. Global Biogeochemical Cycles, 18(4): GB4008
Zhang Wen, White J R, DeLaune R D. 2012. Diverted Mississippi River sediment as a potential phosphorus source affecting coastal Louisiana water quality. Journal of Freshwater Ecology, 27(4): 575–586, doi: 10.1080/02705060.2012.687698
Zhang Jihong, Wu Wenguang, Li Yuchen, et al. 2022. Environmental effects of mariculture in China: An overall study of nitrogen and phosphorus loads. Acta Oceanologica Sinica, 41(6): 4–11, doi: 10.1007/s13131-021-1909-9
Zhuang Wen, Gao Xuelu, Zhang Yong, et al. 2014. Geochemical characteristics of phosphorus in surface sediments of two major Chinese mariculture areas: The Laizhou Bay and the coastal waters of the Zhangzi Island. Marine Pollution Bulletin, 83(1): 343–351, doi: 10.1016/j.marpolbul.2014.03.040

Supplementary information:

Table S1. Hydrochemical characteristics of the water column.

Table S2. Geochemical characteristics of the suspended particulate matter and surface sediment.

Table S3. Grain size of the surface sediment.

The supplementary information is available online at https://doi.org/10.1007/s13131-023-2235-1 and http://www.aosocean.com/. The supplementary information is published as submitted, without typesetting or editing. The responsibility for scientific accuracy and content remains entirely with the authors.